

Potential Application of Membrane Obtained from Sisal Bagasse in the Removal of Inhibitors from the Fermentation Process

Franklin D. Xavier,^a Aleir J. O. Silva,^a Marcos S. Lima,^b Maria G. da Fonseca^c and Marta M. da Conceição^{ib}*,^d

^aPPGQ/CCEN, Universidade Federal da Paraíba, 58051-970 João Pessoa-PB, Brazil

^bInstituto Federal do Sertão Pernambucano, 56316-686 Petrolina-PE, Brazil

^cDepartamento de Química, Universidade Federal da Paraíba, 58051-970 João Pessoa-PB, Brazil

^dDepartamento de Tecnologia de Alimentos, Centro de Tecnologia e Desenvolvimento Regional, Universidade Federal da Paraíba, Av. dos Escoteiros, sn. Mangabeira VII, 58058-600 João Pessoa-PB, Brazil

Annual world production of sisal is estimated to be 400,000 tons, but the processing of sisal fiber generates around 160,000 tons of waste *per* year. The sisal bagasse is discarded, even though it is about 60% carbohydrates in its structure. Therefore, this work seeks to add value to sisal bagasse through the production of cellulose acetate membranes aimed at removing inhibitors from the fermentation process. The membrane was developed using a cellulose acetate polymer synthesized from cellulose isolated from sisal bagasse. Alkaline and acid pre-treatments resulted in 90% pure cellulose. The obtained cellulose acetate was confirmed by infrared spectroscopy. In the synthesis of the membranes, the influence of agitation time and temperature of the bath on the selectivity and porosity were evaluated in four tests, the third condition stood out with porosity of 26.23% and selectivity of 94.51% in the removal of the furfural and 36.62% of the acetic acid.

Keywords: sustainability, lignocellulosic residue, cellulose acetate, furfural, acetic acid

Introduction

The use of renewable resources is a priority in several areas of research due to the scarcity of fossil fuels and the growth of environmental concerns, resulting in increased attention to bioenergy and chemicals derived from biomass in recent years.¹ Lignocellulosic compounds are one of nature's most abundant renewable organic resources. In this context, sisal (*Agave sisalana*) stands out due to its biodegradability,² renewable nature, and a growing number of industrial applications in various sectors.³

Sisal is a well-known source of hard fiber for the textile, alcohol, and composite industries, with an estimated annual production of 400,000 tons worldwide. It is a tropical plant resistant to dry and hot climates and well adapted to semi-arid climates.^{4,5} About 5% of the total mass of sisal is used in fiber production. The residue from this process, known as sisal bagasse, has a high carbohydrate composition.^{6,7}

Lignocellulosic compounds are constituted by a complex formed by cellulose, hemicellulose, and lignin. Because these compounds are lignocellulosic, their components must be selectively separated in order to use them. Pre-treatments can be chemical, physical, thermal, biological, or a combination thereof. The use of pre-treatments is a widespread, low-cost technique that promotes the release of pentoses and hexoses. From the solubilization of the present sugars, biotechnological conversion into xylitol and ethanol in biorefineries is possible.⁸ One of the obstacles to use the hydrolysate for bioconversion is the formation of inhibitors during the biomass hydrolysis process. These products are generated from the decomposition of sugars present in hemicellulose and cellulose under severe conditions of temperature and acid concentration. The main inhibitors are furfural, acetic acid, 5-hydroxymethylfurfural (HMF), and phenolic compounds derived from lignin. These compounds inhibit the metabolism of the microorganism, causing microbial death or reduced productivity.⁹

There are several ways to remove such inhibitors from hydrolysates, where the efficiency of the process

*e-mail: martamaria8@yahoo.com

Editor handled this article: Célia M. Ronconi (Associate)

depends on the raw material, type of pre-treatment, and the microorganism used. Detoxification can be chemical, electrochemical, via membrane separation, and via biological detoxification.¹⁰ Among these methods, membrane separation is a technique that is currently gaining prominence. Membrane separation methods can be classified according to the pore size or the pressure exerted to carry out the experiment; they include reverse osmosis, ultrafiltration, and microfiltration. The use of these techniques has been increasing due to advantages such as low energy consumption, low capital investment, and the recovery of by-products involved in the process.¹¹

Membranes can be classified as organic, inorganic and mixed matrix. Organic membranes are prepared using crystalline or amorphous organic polymers; and vitreous polymers. Most organic membranes are derived from cellulose from biomass. Cellulose is the most abundant homopolymer in nature. Its application extends to several industrial sectors, but, in addition to being used in pure polymeric form, it is also possible to make modifications to its structure to give it new characteristics for other applications.¹² Among the most used modifications is acetylation, also known as the esterification method, which consists of the chemical modification of cellulose, where the three hydroxyl groups of the glucose molecule are replaced by acetyl groups.¹³ By carrying out such modifications, it is possible to obtain greater control over the morphology of the membrane structure due to improvements in the solubility properties of the modified cellulose in solvents with different polarities. This provides variations in experimental arrangements and thus membranes with different morphological properties according to the desired application.¹⁴

The membrane separation process is based on the transport of a chemical species across its surface, for this to occur it is necessary to act on it by a force, which can be a concentration, pressure or electrical gradient. According to the pore size, and the driving force used, it is possible to classify the filtration process. Removal of fermentative inhibitors such as HMF and furfural generally depends on the type of membrane used and the filtration method employed. The methods that are most studied are reverse osmosis, ultrafiltration and nanofiltration.^{12,15}

Membranes derived from cellulose acetate stand out due to their high levels of hardness, biocompatibility, desalination, and flux, along with their relatively low cost. However, membranes synthesized from cellulosic esters are sensitive to thermal and biological degradation.¹⁶ Cellulose derivatives such as cellulose acetate have been gaining prominence within green chemistry because of their high economic value and numerous applications

in the manufacture of membranes, cigarette filters, and cinematographic films, among other products.¹⁷

The objective of the present work was to add value to a lignocellulosic residue through the production of an organic membrane of cellulose acetate that removes inhibitors from the fermentation process. Lignocellulosic materials represent the most significant fraction of plant biomass, and their derivatives provide low environmental impact and the possibility of obtaining various products with high market value such as membranes, biofuels, and other co-products.

Experimental

Materials

The sisal bagasse used in the study came from the municipality of Nova Floresta, in the state of Paraíba, Brazil. The reagents were used without further purification, along with their purity, were sulfuric acid (> 95%, Química Moderna, São Paulo, Brazil), glacial acetic acid (99.7%, Vetec, São Paulo, Brazil), acetic anhydride (97%, Dinâmica, São Paulo, Brazil), dichloromethane (99.5%, Vetec, São Paulo, Brazil), sodium chlorite (> 80%, Sigma-Aldrich, Saint Louis, USA), and sodium hydroxide (97%, Vetec, São Paulo, Brazil).

Determination of lignocellulosic composition

The sisal bagasse was ground in a knife mill, and granulometric distribution was carried out to standardize the material. Following Technical Association of the Pulp and Paper Industry (TAPPI) standards,¹⁸ the main lignocellulosic constituents were determined. The holocellulose, alpha-cellulose, Klason lignin, and ash contents were determined according to TAPPI T19 M-54, TAPPI 203 cm-99, TAPPI 222, and modified TAPPI 413 om-11 standards, respectively. The hemicellulose content was calculated by subtracting the percentage of alpha-cellulose from the holocellulose content.⁴

Cellulose isolation

All chemical pre-treatments were carried out in a Biofoco stainless steel pressurized reactor (São Paulo, Brazil) with an operating volume of 700 mL. The treatments were intended to partially or totally remove the hemicellulosic fraction and biomass delignification.

Acid pre-treatment

To examine the influence of sulfuric acid concentration,

time, and temperature on the solubilization of sugars present in the biomass, a 2³ factorial design was used with three replications at the central point. In the general experimental procedure, the independent variables for the experiments were temperature (100-120 °C), reaction time (30-60 min) and acid concentration (1-3%). All experiments were carried out at a ratio of 1:10 (m/v) sisal/acid solution. The response variables were the concentrations of xylose and glucose obtained in the hydrolyzed liquors, which were quantified using high-performance liquid chromatography (HPLC).¹⁹

High-performance liquid chromatography

Analyses were performed on an Agilent chromatograph, model 1260 Infinity LC (Agilent Technologies, Santa Clara, CA, USA), equipped with a quaternary solvent pump (model G1311C), degasser, thermostated column compartment (model G1316A), and automatic sampler (model G1329B) coupled to a diode array detector (model G1315D) and refractive index detector (RID) (model G1362A).

A 500- μ L aliquot of the hydrolyzed liquor was diluted in 1.0 mL of ultrapure water, filtered through a 0.45- μ m nylon membrane, and a volume of 10 μ L was injected. The ion exchange column was Agilent Hi-Plex H (300 \times 7.7 mm) with 8.0- μ m internal particles and PL Hi-Plex H guard column (5 \times 3 mm) (Agilent Technologies, Santa Clara, CA, USA). The column compartment temperature was maintained at 70 °C, and the RID flow cell was maintained at 50 °C. The applied flow rate was 0.5 mL min⁻¹. The mobile phase was 4.0 mmol L⁻¹ H₂SO₄ in ultrapure water.

Alkaline delignification

The alkaline pre-treatment was carried out in the best condition obtained after analyzing the proposed experimental design. The biomass after acid treatment and a 5% sodium hydroxide (NaOH) solution in the proportion 1:10 (m/v) were inserted into the reactor with a heating ramp until reaching a temperature of 100 °C, using a reaction time of 30 min. The solid fraction was separated from the liquid fraction by vacuum filtration and then washed with distilled water. The material was dried at room temperature and stored.²⁰

Bleaching

The resulting cellulose underwent a bleaching process in order to remove the remaining lignin from the complex. In a polypropylene container, the biomass was mixed with

distilled water in the proportion of 10% (m/v). The mixture was stirred and heated to 70 °C. Subsequently, 3 mL of glacial acetic acid (CH₃COOH) and 3 g of sodium chlorite (NaClO₂) were added. The mixture was stirred and heated for 3 h. Then, the sample was filtered and washed with distilled water.

The effectiveness of the treatment was measured through the parameters of lignocellulosic composition and Kappa number. The methodology used to determine the Kappa number followed the Brazilian standard ABNT NBR ISO 302:2018 for cellulosic pulps.²¹

Synthesis of cellulose acetate

From the recovered sisal bagasse cellulose, the synthesis of cellulose acetate was carried out using the methodology described by Candido *et al.*²⁰ First, 24 mL of glacial acetic acid was added to 10 g of sisal bagasse cellulose, and then this mixture was stirred at 38 °C for 1 h. Then, 40 mL of glacial acetic acid and 0.08 mL of sulfuric acid were added to the mixture, which was stirred for 45 min. Then, the mixture was cooled to room temperature, and 28 mL of acetic anhydride and 0.6 mL of sulfuric acid were added. The temperature was raised to 38 °C, and the mixture was stirred for 1.5 h. Finally, the obtained material was filtered and washed with distilled water. The cellulose acetate precipitate was dried in an oven at 50 °C for 6 h and characterized by infrared absorption spectroscopy.

Production of membranes

To evaluate the influence of the temperature of the non-solvent and the agitation time on the dissolution of the polymeric matrix, four conditions for the synthesis of cellulose acetate membranes were studied (Table 1). The solutions were prepared using cellulose acetate from sisal bagasse, following the phase inversion method. First, 3 g of the material were weighed, and 50 mL of dichloromethane were added and stirred. Then, the solution was degassed in an ultrasonic bath to remove air bubbles. Next, the solution was spread on a glass plate that, after the solvent had

Table 1. Experimental conditions for the synthesis of cellulose acetate membranes

Membrane	Shaking time / h	Coagulation bath temperature / °C
M1	4	5
M2	4	25
M3	5	5
M4	5	25

evaporated, was immersed in a coagulation bath containing distilled water for 2 h or until the phase inversion process was completed.^{22,23}

The experimental parameters adopted in this research were based on Candido *et al.*,¹⁷ Xavier *et al.*,¹⁹ Candido *et al.*²⁰ and Upadhyaya *et al.*²² In these references, the polymers used as raw material showed similar properties to cellulose acetate produced from sisal bagasse. Thus, they were used as initial research conditions.

Characterization of membranes

The produced membranes were characterized according to their physical properties and selectivity through scanning electron microscopy (SEM), porosity, permeated water vapor flow, and removal of sugars and inhibitors.

Porosity

The membrane was initially impregnated with distilled water and weighed after drying its surface water. Subsequently, the wet membrane was placed in an air circulation oven at 80 °C for 24 h until it reached constant mass.²⁴ The dry membrane was weighed and the porosity calculated using equation 1:

$$P(\%) = \left(\frac{Q_0 - Q_1}{A \times h} \right) \times 100 \quad (1)$$

where P: membrane porosity; Q_0 : wet membrane weight (g); Q_1 : dry membrane weight (g); A: membrane surface area (cm²); and h: membrane thickness (mm).

Flow of water vapor

To determine the permeated water vapor flow, the methodology of Candido *et al.*¹⁷ was applied using a Payne cup. The membranes were cut into discs with a diameter equal to the container. The set was assembled with distilled water occupying 50% of the volume of the beaker, weighed on an analytical scale, and inserted into a desiccator. The system mass variation was monitored in the 1-hour interval between weighings. From the data obtained, a graph of mass variation as a function of time was constructed. By means of linear regression, the equation of the straight line was obtained, in which the value of the angular coefficient was used to calculate the water vapor flow by equation 2:

$$J = \frac{\Delta m}{\Delta t} \frac{1}{A} \quad (2)$$

where J: mass flux of water vapor (mg h⁻¹ cm⁻²); Δm : change

in mass (mg); Δt : time variation (h); and A: membrane area (cm²).

Removal of sugars and inhibitors

Membranes synthesized from cellulose acetate from sisal bagasse were characterized in terms of their ability to remove inhibitors from the fermentation process, using a “dead end” filtration system. The tests were performed using a fixed pressure of 1 bar. Initially, acid hydrolysis of the untreated material was performed using 3% sulfuric acid at a temperature of 140 °C. Then, an aliquot was removed for chromatographic analysis. This hydrolysate was used in the removal tests for all synthesized membranes. At the end of the tests, the permeate solutions were analyzed by HPLC to determine the concentration of sugars and inhibitors and thus to calculate the percentage of removal in the cellulose acetate membranes.

The filtration module used in this research is of the “dead end” type, a class of modules whose operation occurs when a current containing the analyte (what you want to separate) passes through it and from there accumulates on the surface and in the inside the filter medium (membrane). The equipment used to analyze the properties of the synthesized membranes it refers to a vertical “dead end” module coupled to a pump to pressurize the system at constant pressure.

General methods

Absorption spectroscopy in the infrared region

Treated and untreated samples were analyzed by Fourier transform infrared spectroscopy (FTIR) on a Shimadzu IR Prestige Spectrophotometer (Japan), using KBr in the range of 4000-400 cm⁻¹.

Scanning electron microscopy (SEM)

The morphology and the change in the physical structure of the synthesized membranes were evaluated by SEM. The samples were cut into squares measuring about 1 cm² and metallized with gold. The analysis was carried out in SEM Quanta Fei 450-EDS BRUKER 30 (Czech Republic) at a voltage of 5 kV.

Results and Discussion

Statistical analysis of acid pre-treatment

Isolation of cellulose with the lowest presence of hemicellulose and lignin implies using fewer steps for delignification and purification in order to obtain purer cellulose at the end of the recovery process. First, the acid

Table 2. Factorial design and experimental values of xylose, glucose, and acetic acid concentrations for sisal bagasse

Experiment	Concentration / %	Temperature / °C	time / min	Xylose / (g L ⁻¹)	Glucose / (g L ⁻¹)	Acetic acid / (g L ⁻¹)
1	1	100	30	0.17	1.51	0
2	3	100	30	0.43	1.46	0
3	1	120	30	0.91	1.54	0
4	3	120	30	3.55	2.82	0.42
5	1	100	60	0.16	1.40	0
6	3	100	60	0.98	1.56	0
7	1	120	60	1.26	1.62	0
8	3	120	60	3.71	3.04	0.45
9	2	110	45	1.89	1.87	0.58
10	2	110	45	1.74	1.82	0.73
11	2	110	45	1.37	1.64	0

treatment was conducted by removing the hemicellulosic fraction.^{25,26} When carrying out the acid pre-treatment under conditions described in Table 2, hydrolysate was produced and then separated by filtration, and a solid fraction was washed and dried for the delignification step. Aliquots were taken from the hydrolyzed liquor for HPLC analysis (Table 2).

It was found that condition 8 of the factorial design (3% sulfuric acid concentration at 120 °C for 1 h) solubilized the highest concentration of xylose and glucose, in addition to producing a small amount of acetic acid. This is considered an important parameter since acetic acid is one of the inhibitors of the fermentation process in the conversion of hydrolyzed liquor into, for example, ethanol or xylitol. The hydrolyzed liquor in the best condition of sisal bagasse presented 3.71 g L⁻¹ of xylose and 3.04 g L⁻¹ of glucose.

The experimental results were statistically analyzed by analysis of variance (ANOVA) and linear regression analysis to define the best acid treatment conditions for the solubilization of pentoses and removal of hemicellulose from the structure. Table 3 describes the equations that would reproduce the xylose and glucose concentrations as predicted by the model as a function of the coded variables. The parameterized model contains only statistically significant terms at 95% confidence, as well as the respective coefficients of determination (R²) and the values of the *F*-test.

Table 3. Linear regression models for the response variables xylose and glucose

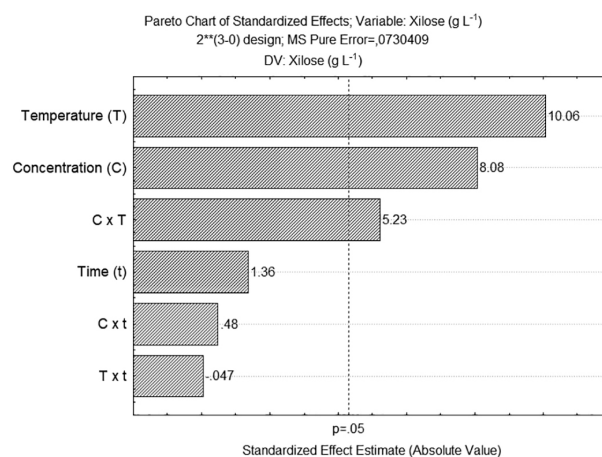
Regression model	R ²	<i>F</i> -test
Xylose = 1.47 + 0.77C + 0.96T + 0.49CT	96.41	14.81
Glucose = 1.84 + 0.35C + 0.39T + 0.32CT	97.20	18.64

C: H₂SO₄ concentration; T: temperature; t: time; R²: coefficient of determination.

According to the equations presented in Table 3, the linear models of sisal bagasse are statistically significant for xylose and glucose because they present a ratio *F*_{calculated}/*F*_{tabled} greater than 1.¹⁹ The model for xylose removal showed a 96.41% coefficient of determination and an *F*-test equal to 14.81, indicating statistical significance with 95% confidence.

The Pareto chart is widely used to represent the significance of parameters and their interactions in experimental designs. In Figure 1, the horizontal bars display the importance of the input variables for the proposed experimental design in descending order. Any parameter that crosses the dashed line is considered significant according to the confidence level adopted, which in this case was 95% or α of 0.05.²⁵ The Pareto diagram was obtained when performing the statistical analysis of the data for the concentration of removed sugars (Figure 1).

As seen in the Pareto chart, the increase in xylose removal was significantly affected by the increase in acid

**Figure 1.** Pareto diagram for the concentration of xylose removed from sisal bagasse.

concentration and temperature, with a positive value for the effects. In this case, time did not significantly influence xylose removal. Regarding the interactions between the variables, only the interaction between concentration and temperature was statistically significant. Thus, the concentration of xylose removed from the sisal bagasse increased as the acid concentration and temperature increased, up to the maximum condition of the range studied. According to the analysis of the effects shown in the Pareto diagram and in the experimental matrix, condition 8 was the best test to hydrolyze the sugars present in the hemicellulose.

Lignocellulosic composition

Untreated sisal bagasse had a lignocellulosic composition of 36.09% cellulose, 21.46% hemicellulose, 12.11% lignin, and about 21% ash and extractives. The results are corroborated by data in the literature. In Lima *et al.*²⁶ work with sisal as a source of biomass, the sisal bagasse had a cellulose content of 27.6% and hemicellulose content of 20.6%, about 8% lower than the data obtained in the present work. After acid and alkaline pre-treatments in the current study, the sisal bagasse had a lignocellulosic composition of 59.77% cellulose, 9.89% hemicellulose, 5.15% lignin, and about 8.24% ash and extractives.

Regarding the percentage of cellulose, there was an increase in the cellulose content of 59.77%, indicating that the resulting material had the most exposed cellulose and had not undergone hydrolysis by acid attack; regarding the percentage of lignin, there were lower values present in the complex. The glucose concentration present in the hydrolyzed liquor is possibly derived from the hemicellulose structure and the most amorphous part of cellulose.²⁷ The diluted acid pre-treatment helps to increase the percentage of cellulose in the raw materials. The effectiveness of the pre-treatment can be evaluated by removing hemicellulose and lignin components, in addition to improving surface accessibility to cellulose.⁹

The alkaline treatment removed about 58% of the lignin. According to Ismail *et al.*,²⁸ studying of the effect of NaOH concentration in alkaline pre-treatment in different biomass species, the final composition of the residue was affected by concentrations above 5% (m/v). Láinez *et al.*,⁵ working on the alkaline delignification of sisal fiber to produce fermentable sugars, used a NaOH concentration of 4% (m/v) and obtained about 60% lignin removal, reflecting very similar results to those observed in the present work.

The Kappa number, calculated for the pulp sample obtained under the best conditions, was found to be 26.63. The Kappa number is an experimental value that determines

the percentage of non-cellulose components present in the sample. Comparing the Kappa number and the lignin contents, it was verified that the sisal bagasse had a low lignin value at the end of the pre-treatments.

The choice of delignification method used can affect the final pulp obtained due to the possibility of lignin being decomposed into different products. In alkaline medium, cleavage of the structure's ester bonds occurs, generating free phenolic groups. The resulting lignin fragments are water-soluble and can be easily isolated from the liquor through precipitation.²⁸ Thus, a bleaching step was necessary for a purer cellulose that was free from interferences for its acetylation step.

The cellulose is preserved in the bleaching step while hemicellulose and lignin are solubilized in this process.¹⁷ In the present study, the cellulose of the sisal bagasse obtained a Kappa number of 9.18 after the bleaching process, which was lower than the sample from the previous step. Although there were still other components in addition to the cellulose from the sisal bagasse, the value obtained for the Kappa number after bleaching is within the standard found in the literature. Obtaining membranes derived from sugarcane bagasse, Candido *et al.*²¹ bleached the samples before modifying their structure and, in the best condition, found a Kappa number close to 15.

Obtaining cellulose acetate

The cellulose sample obtained was acetylated using homogeneous acetylation, and the resulting cellulose acetate was evaluated by FTIR. The spectra obtained for the bleached cellulose and the cellulose acetate were then compared (Figure 2).

From the acetylation reaction, it was possible to obtain several mono-, bi-, and tri-substituted compounds. Several

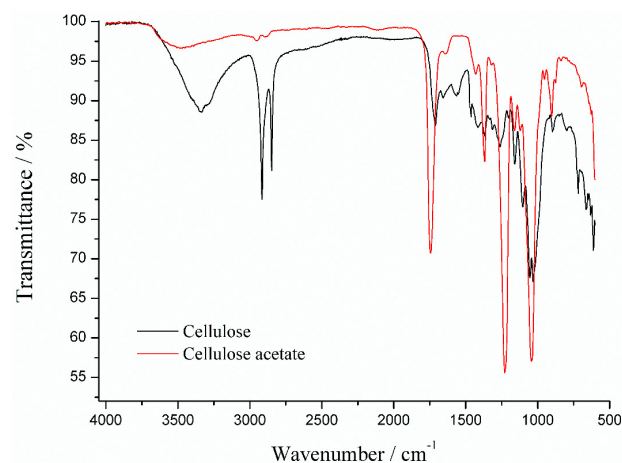


Figure 2. FTIR (KBr) spectra of cellulose and cellulose acetate synthesized from sisal bagasse cellulose.

factors can affect the degree of substitution including temperature, concentration of reagents, and time. Analyzing the infrared spectra, four changes in the structure that characterize the formation of cellulose triacetate stand out: the appearance of three new bands and the reduction in the transmittance intensity in the region of 3330 cm^{-1} .²⁸⁻³⁰ The reduction in intensity in this region is caused by the reduction of hydroxyls in cellulosic chains since the acetylation reaction causes the replacement of hydroxyls by acetyl groups. As a result of the replacement of these functional groups, bands referring to ester bonds and the acetyl group appear. At the same time, there was a reduction in the region of 2914 cm^{-1} which represents the typical C–H bond elongation of the cellulose molecule.²¹ The region situated at 1750 cm^{-1} refers to the carbonyl (C=O) stretch of esters; 1370 cm^{-1} refers to C–H strain and 1230 cm^{-1} refers C–O stretch in acetyl groups.¹⁴ In the spectrum, a band at 1040 cm^{-1} was observed, which can be attributed to $\text{O}=\text{C}-\text{O}-\text{CH}_3$.²¹ The variations shown indicate the replacement of hydroxyl groups by acetyl groups occurring in the acetylation process.³¹

Characterization of cellulose acetate membranes

The cellulose acetate membrane was prepared using the phase inversion method, which ensures greater stability and control for membranes derived from biomass, mainly due to the use of low synthesis temperatures. There are several parameters that affect the formation of the membrane structure: choice of solvent, mass ratio of polymer/solvent, concentration and evaporation time before immersion in the bath, and bath temperature.²² The cellulose acetate membranes produced in the present study had a firm surface and were opaque and flat, with an average thickness of 0.16 mm (Figure 3).

Membrane morphology indicates formation differences during the synthesis process. The cellulose acetate membrane formed in all cases had an asymmetric structure. The upper surface of the membrane was denser on membranes M1 and M3, where the coagulation bath temperature was $5\text{ }^\circ\text{C}$. In the M4 condition, the surface of the cellulose acetate membrane was irregular, unlike the M3 membrane. Assays M4 and M3 presented morphologies that

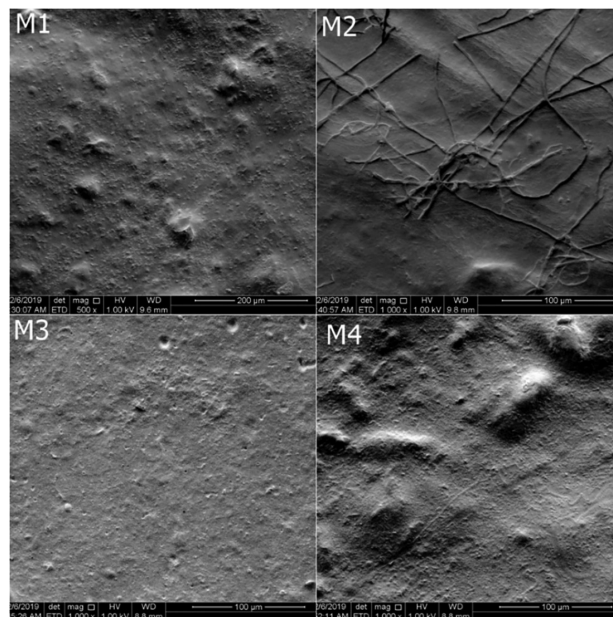


Figure 3. Micrographs of cellulose acetate membranes.

suggest that the temperature of the coagulation bath was not a determining factor in their structure. This was confirmed by the fact that in membranes M1 and M2, which had shorter agitation times, the polymeric matrix was not completely dissolved in the solvent, leaving clusters of polymers that did not react during the phase inversion process and were encrusted on the surface of the membranes. This finding suggests that stirring time is a determining factor in the morphology of the membranes. This morphology is in line with the findings of Meireles *et al.*³² and Vatanpour *et al.*,³³ who noted that the presence of lignin fragments affected the interactions between the polymeric chains, resulting in regions of low density in the polymer.

The porosity analysis determined the percentage of pores present in the membrane structure. It was found that the four membranes were porous, corroborating the morphological structure data. However, it should be noted that this percentage is not related to the pore size or its distribution in the structure.¹⁷ Data on physical properties and removal rates of inhibitors from the fermentation process are shown in Table 4.

Comparing the porosity and water vapor flow data shows inversely proportional values between the membranes, that

Table 4. Physical parameters and performance of cellulose acetate membranes

Membrane	Porosity / %	Water vapor flow / ($\text{mg h}^{-1}\text{ cm}^2\ \mu\text{m}^{-1}$)	Removal of furfural / %	Acetic acid removal / %
M1	12.92	1.44×10^{-2}	81.88	17.92
M2	9.85	5.79×10^{-2}	77.23	22.93
M3	26.23	1.16×10^{-2}	94.51	36.62
M4	22.07	2.99×10^{-2}	90.54	5.55

is, the greater the porosity, the lower the water vapor flow (Table 4). The porosity indicates only the amount of pores, but when related to the amount of permeated vapor, show the M3 membrane had the highest percentage of pores (26.23%) among the produced membranes, which probably have a smaller pore size compared to those synthesized in other assays.³⁴ In addition, we may infer that the solvent agitation time was the parameter that most influenced the formation of pores in the membrane structures. More time spent stirring the solvent led to greater porosity. The longer stirring time led to greater compaction of the cellulose acetate chain and consequently greater pore formation. On the other hand, temperature was not an impacting factor since membranes synthesized with identical temperatures such as M1 and M3 presented very different values.

All membranes showed water vapor flux, and M2 and M4 membranes, which had a higher coagulation bath temperature, showed higher flux. This longer agitation time allowed the formation of a more uniform membrane, promoting the passage of solvent more directly through the membrane. Despite having the lowest porosity, the M2 test had the highest water vapor flow ($5.79 \times 10^{-2} \text{ mg h}^{-1} \text{ cm}^{-2} \mu\text{m}^{-1}$), confirming that pore arrangement is a determining factor for the passage of water vapor through the membrane.³² Other authors that used biomass to produce membranes, such as Meireles *et al.*,³² mentioned similar values for the permeate water flux. These authors used membranes derived from mango seed biomass, obtaining value of $3.11 \times 10^{-5} \text{ g s}^{-1} \text{ cm}^{-2}$.

Comparison of the membranes revealed that increasing the stirring time and decreasing the temperature of the coagulation bath increased the porosity of the membrane. Thus, the phase inversion rate was increased, which increased the thermodynamic instability of film formation during the phase inversion process. Membranes with similar synthesis parameters (M3 and M4) did not show great difference in their porosity percentages (around 4%), as observed in M1 and M2 membranes, which also presented values close to each other.

Performance evaluation of cellulose acetate membranes

The hydrolyzed liquor used to evaluate the performance of the membranes regarding the removal of sugars and inhibitors from the fermentation process presented 5.39 g L^{-1} glucose, 11.09 g L^{-1} xylose, 4.10 g L^{-1} acetic acid, and 5.57 g L^{-1} furfural. Among the tested membranes, the M3 membrane showed the highest percentage of removal of inhibitors, with 94.51% removal of furfural and 36.62% of acetic acid. Table 4 shows that all membranes showed excellent results for furfural reduction (M1: 81.88%;

M2: 77.23%; M4: 90.54%) when compared with other works. Ozay *et al.*³⁵ studied the use of commercial membranes in ultra and nanofiltration processes for the recovery of acetic acid in wastewater, obtaining rejection of 39.6%, a value very similar to that found for the M3 membrane. Sawatdiruk *et al.*³⁶ obtained 75.6% selectivity in furfural recovery using membrane separation. In general, all membranes showed lower results for acetic acid selectivity when compared to furfural selectivity; however, these values are similar to other separation techniques employed: distillation, precipitation, liquid-liquid recipe and adsorption.³⁴

As for the physical properties and retention values, the synthesis parameters with longer agitation time and lower temperature produced membranes with better furfural and acetic acid removal values. Factors such as concentration of analytes in the solution to be tested, pore size, and physical-chemical interactions can define the efficiency of the separation process.³³

The M3 membrane had greater porosity and almost non-existent roughness on its surface, resulting in greater removal of inhibitors. The M4 and M1 membranes had remnants of other polymeric components, which hindered their pore distribution and consequently the removal of sugars. A justification for the membranes produced in these studies to present different morphologies is the synthesis method used. Membranes synthesized by the phase inversion method tend to be asymmetrical and present different morphologies. Khan *et al.*³⁷ mentions that the greater interaction between the coagulation bath and the polymeric solution causes a more uniform pore size distribution and high porosity in the membrane structure. This method is the most applied for cellulose acetate derivatives where changing phase inversion conditions, such as cellulose acetate concentration, type of solvent, coagulation bath temperature, addition of different additives, it is possible to prepare membranes with different pore sizes, morphologies and applications.³⁵

The initially characterized membranes showed high permeate water flux and porosity. According to their physical characteristics and high selectivity for inhibitory compounds, these membranes would be suitable for micro or ultrafiltration processes. Membranes derived from lignocellulosic biomass can be applied in various filtration methods, where their application is related to the synthesis method used, degree of purity, cellulose crystallinity, and chemical modification.¹¹

Conclusions

Cellulose acetate membranes obtained from sisal bagasse were successfully synthesized. After the pre-treatment and

bleaching steps, the isolated cellulose showed about 10% of other lignocellulosic components remaining, mainly impairing the synthesis of the M2 membrane. Infrared spectra confirmed the replacement of free OH groups by acetyl groups and formation of cellulose acetate. The synthesized membranes showed good mechanical characteristics, supporting pressures above 1 bar.

According to the synthesis parameters studied, the agitation time was the factor that most influenced the performance of the membranes. Membranes M3 and M4, which were produced with longer stirring times, showed higher percentages of removal of furfural and acetic acid. The M2 membrane showed the best water vapor flow ($5.79 \times 10^{-2} \text{ mg h}^{-1} \text{ cm}^{-2} \mu\text{m}^{-1}$) while M3 showed the highest percentage of pores (26.23%). Thus, the M3 membrane demonstrated the best performance among the synthesized membranes, both in terms of its physical properties and its selectivity in the removal of furfural from the lignocellulosic hydrolysate, with 94.51% removal.

In view of the data obtained, the cellulose acetate membranes synthesized from sisal bagasse can be applied in processes of separation, concentration, purification, and drug release, among others. Sisal bagasse is a renewable raw material, constituting an agro-industrial waste with a high carbohydrate content in its structure. In this way, the synthesized membrane presents low production cost, added value to a waste discarded in nature, and an efficient method for removing inhibitors from the fermentation process, thus contributing to environmental sustainability.

References

- Reis, A. M. S.; Vieira, A. T.; Santos, A. L. R.; Ferreira, M. V.; Batista, A. C. F.; Assunção, R. M. N.; Rodrigues Filho, G.; Ribeiro, E. A. M.; Faria, A. M.; *J. Braz. Chem. Soc.* **2020**, *31*, 1011. [Crossref]
- Choudhary, S.; Sain, M. K.; Kumar, V.; Saraswat, P.; Jindal, M. K.; *Mater. Today: Proc.* **2023**. [Crossref]
- Tesfay, D.; Balakrishnan, S.; Ashine, F.; Sivaprakasam, P.; *Mater. Today: Proc.* **2022**, *62*, 448. [Crossref]
- de Oliveira, F.; da Silva, C. G.; Ramos, L. A.; Frollini, E.; *Ind. Crops Prod.* **2017**, *96*, 30. [Crossref]
- Láinez, M.; Ruiz, H. A.; Castro-Luna, A. A.; Martínez-Hernández, S.; *Biomass Bioenergy* **2018**, *118*, 133. [Crossref]
- Castoldi, R. S.; de Souza, L. M. S.; Souto, F.; Liebscher, M.; Mechtcherine, V.; Silva, F. A.; *Constr. Build. Mater.* **2022**, *345*, 128363. [Crossref]
- Yang, Y.; Yang, J.; Cao, J.; Wang, Z.; *Bioresour. Technol.* **2018**, *267*, 517. [Crossref]
- Mariño, M. A.; Cypriano, D.; Tasic L.; *J. Braz. Chem. Soc.* **2021**, *32*, 878. [Crossref]
- Kang, S.; Fu, J.; Zhang, G.; *Renewable Sustainable Energy Rev.* **2018**, *94*, 340. [Crossref]
- Rao, L. V.; Goli, J. K.; Gentela, J.; Koti, S.; *Bioresour. Technol.* **2016**, *213*, 299. [Crossref]
- Favvas, E. P.; Katsaros, F. K.; Papageorgiou, S. K.; Sapalidis, A. A.; Mitropoulos, A. C.; *React. Funct. Polym.* **2017**, *120*, 104. [Crossref]
- El-Gendi, A.; Abdallah, H.; Amin, A.; Amin, S.; *J. Mol. Struct.* **2017**, *1146*, 14. [Crossref]
- Chen, J.; Xu, J.; Wang, K.; Cao, X.; Sun, R.; *Carbohydr. Polym.* **2016**, *137*, 685. [Crossref]
- Daud, W. R. W.; Djuned, F. M.; *Carbohydr. Polym.* **2015**, *132*, 252. [Crossref]
- Bozic, M.; Vivod, V.; Kavcic, S.; Leitgeb, M.; Kokol, V.; *Carbohydr. Polym.* **2015**, *125*, 340. [Crossref]
- Battirola, L. C.; Andrade, P. F.; Marson, G. V.; Hubinger, M. D.; Gonçalves, M. C.; *Cellulose* **2017**, *24*, 5593. [Crossref]
- Candido, R. G.; Godoy, G. G.; Gonçalves, A.; *Carbohydr. Polym.* **2017**, *167*, 280. [Crossref]
- Testing Procedures of Technical Association of the Pulp and Paper Industrial (TAPPI); *TAPPI Standard Method*, Atlanta. [Link] accessed in April 2023
- Xavier, F. D.; Bezerra, G. S.; Florentino, S. M. S.; Oliveira, L. S. C.; Silva, F. L. H.; Silva, A. J. O.; Conceição, M. M.; *Biomolecules* **2018**, *8*, 2. [Crossref]
- Candido, R. G.; Gonçalves, A. R.; *Carbohydrate Polymers* **2016**, *152*, 679. [Crossref]
- ABNT NBR ISO 302:2018: *Pastas Celulósicas - Determinação do Número Kappa*, Rio de Janeiro, 2018.
- Upadhyaya, L.; Semsarilar, M.; Nehache, S.; Deratani, A.; Quemener, D.; *Eur. Phys. J.: Spec. Top.* **2015**, *224*, 1883. [Crossref]
- Mirkhalili, S. M.; Mousavi, S. A.; Saadat Abadi, A. R.; Sadeghi, M.; *Korean J. Chem. Eng.* **2017**, *34*, 3170. [Crossref]
- Ghaemi, N.; Khodakarami, Z.; *Carbohydr. Polym.* **2019**, *204*, 78. [Crossref]
- Ferreira, S. L. C.; Caires, A. O.; Borges, T. S.; Lima, A. D. S.; Silva, L. O. B.; dos Santos, W. N. L.; *Microchem. J.* **2017**, *131*, 163. [Crossref]
- Lima, C. S. S.; Conceição, M. M.; Silva, F. L. H.; Lima, E. E.; Conrado, L. S.; Leão, D. A. S.; *Appl. Energy* **2013**, *102*, 254. [Crossref]
- Mood, S. H.; Golfeshan, A. H.; Tabatabaei, M.; Jouzani, G. S.; Najafi, G. H.; Gholami, M.; Ardjmand, M.; *Renewable Sustainable Energy Rev.* **2013**, *27*, 77. [Crossref]
- Ismail, S.; Saharuddin, M. Q.; Zahari, M. S. M.; *Energy Procedia* **2017**, *138*, 372. [Crossref]
- Upton, B. M.; Kasko, A. M.; *Chem. Rev.* **2016**, *116*, 2275. [Crossref]
- Saiful; Hasima, S.; Kamila, N.; Rahmi; *Results Eng.* **2022**, *15*, 100611. [Crossref]

31. Peredo, K.; Reyes, H.; Escobar, D.; Vega-Lara, J.; Berg, A.; Pereira, M.; *Carbohydr. Polym.* **2015**, *117*, 1014. [Crossref]
32. Meireles, C. S.; Rodrigues Filho, G.; Ferreira Jr., M.; Cerqueira, D.; Assunção, R. M. N.; Ribeiro, E. A. M.; Poletto, P.; Zeni, M.; *Carbohydr. Polym.* **2010**, *80*, 954. [Crossref]
33. Vatanpour, V.; Pasaoglu, M. E.; Barzegar, H.; Teber, O. O.; Kaya, R.; Bastug, M.; Khataee, A.; Koyuncu, I.; *Chemosphere* **2022**, *295*, 133914. [Crossref]
34. Vetrivel, S.; Saraswathi, M. S. A.; Rana, D.; Nagendran, A.; *Int. J. Biol. Macromol.* **2018**, *107*, 1607. [Crossref]
35. Ozay, Y.; Isik, Z.; Dizge, N.; *J. Water Process Eng.* **2020**, *38*, 101532. [Crossref]
36. Sawatdiruk, S.; Charoensuppanimit, P.; Faungnawakij, K.; Klaysom, C.; *Sep. Purif. Technol.* **2022**, *278*, 119281. [Crossref]
37. Khan, B.; Zhan, W.; Lina, C.; *J. Appl. Polym. Sci.* **2020**, *137*, 49556. [Crossref]

Submitted: January 6, 2023

Published online: May 3, 2023

